Chapter 7

Raman spectra of liquid carbon disulfide

Carbon disulfide (CS_2) is the liquid studied most intensively by nonlinear Raman spectroscopy both experimentally [36, 37, 39–41, 45, 69, 74, 75, 81, 170–176] and theoretically. [55, 56, 58, 70, 77, 95, 96, 104, 105, 126, 133, 177–183] This is mainly due to the large polarizability and especially the large anisotropy in the polarizability of the carbon disulfide molecule. This results in a strong response, both for intermolecular modes and molecular reorientational motions, which makes carbon disulfide a favorable liquid to study.

In this chapter calculations on carbon disulfide are presented. These calculations were used to test the new finite field method described in chapter 3. This was done by comparing the third-order finite field results to results obtained with the time correlation function method. Furthermore the importance of the local field effects, discussed in chapter 4 and examined for dimers in chapter 5, were investigated in particular for the third-order response.

The fifth-order response was calculated using the finite field method. First, as will be described in section 7.3, this was done with the molecular polarizability model (MOL), described in chapter 4 and 5, giving a first estimate of the intensity of the true fifth-order signal. This absolute intensity of the response was compared with that expected for the competing third-order cascades as described in section 2.4, allowing us to give the first estimate of the ratio between the true and the cascaded fifth-order response. Then, the more accurate dipole-induced dipole model (DID) that includes a large part of the intermolecular response was used to give a more precise estimate of the intensity. This also allows investigating the difference between the various polarization directions. These

calculations are presented in section 7.4. Finally the direct reaction field model (DRF) that was optimized to the time-dependent density functional theory calculations as described in chapter 5, was used to give the best possible calculation of the fifth-order response allowing a first comparison with the most recent experiments in section 7.5.

7.1 The finite field method

In the first calculations with the finite field method [55] the molecular model for the first-order susceptibility (MOL) described in section 4.2 was used. This model had the advantages that the calculations were fairly rapid to perform and the computer code was rather simple. The model also implies that there is only one component of the response to consider, since independent molecules do not give rise to an isotropic response. Including only the single molecule (reorientational) motion is reasonable as a first approximation, since this motion is known to dominate the long diffusive tail observed in the third-order spectrum. The finite field response was obtained from 8000 simulations of 2 ps duration. The strength of the applied laser field was 0.383 V/Å. At this magnitude the response was found to be stong enough to separate from numerical noise and the higher order response weak enough to be neglected. This field stength was chosen after investigations on a wide range of field strengths. The correlation function response was obtained from a single simulation of 100 ps duration. The simulation box contained 256 molecules and the further simulation conditions were as described in chapter 6. In Figure 7.1 the calculated third-order response functions are compared with each other and with the experimental response function. [82]

In the comparison between the third-order responses, calculated using the equilibrium MD correlation function approach and the non-equilibrium finite field approach, almost perfect agreement is observed (Figure 7.1). The long diffusive tail of the experimentally observed signal is reproduced very well by both calculated response functions. The discrepancy with the experiment at short times is due to the neglect of local field effects. Previous correlation function calculations of the same third-order response function by Geiger and Ladanyi [96] have also shown that the long diffusive tail is well reproduced, even when one omits the local field effects. However, the peak at 200 fs is underestimated by a factor of 2 by not taking these effects into account. The comparison of our results with those of Geiger and Ladanyi [96] indicate that inclusion of local field effects in our calculations will give results in much better agreement with the experiment at short times.

FIGURE 7.1: *Third-order Raman response $\chi^{(3)}_{zzzz}$ of CS_2, calculated using the finite field method and the correlation function method employing the molecular approximation (MOL) of the first-order susceptibility. The experimental response [82] is also shown, scaled such that the tail overlaps the calculated tails.*

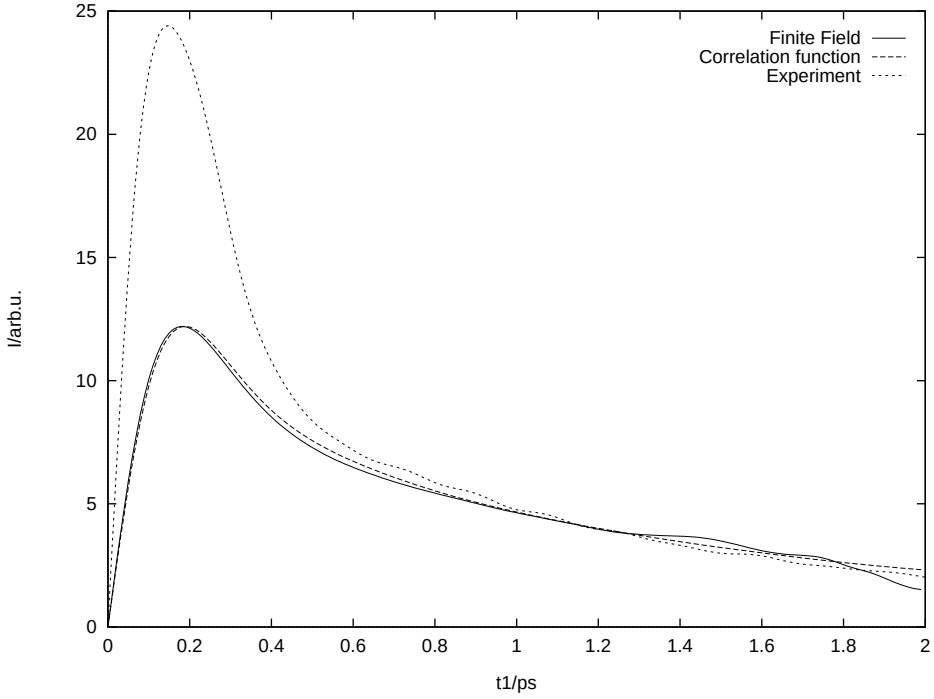

The finite field method used in the above calculations was proven to be reliable. This conclusion is based on the agreement between the third-order response functions calculated with the finite field method and the correlation function method. The finite field method can therefore also be applied with confidence for calculations that include local field effects and for the fifth-order calculations. This new method is a bit more time consuming in the present third-order calculations, but this is mainly due to the fact the correlation function can be simplified when local field effects are ignored.

7.2 Local field effects

Calculations on the third-order Raman response of CS_2 were also performed [62] using the DRF method, described in chapter 4, to include the local field effects. The cut-off distance beyond which the local field interactions are not taken into account was set to 20 Å and the interaction was softly reduced over a 0.2 Å thick region, using the method described in section 4.4. The simulated box contained 64 molecules and the simulations were repeated 10000 times to ensure high accuracy. The strength of the applied laser fields was 1.149 V/Å.

Calculations containing only the DID effect (DID), the pure multipole model (POL) and the DRF model including multipole and electron overlap effects (DRF) were performed. The anisotropic responses are shown in Figure 7.2. Comparing the single molecule result (MOL) of the previous section with the other responses makes clear that the subpicosecond peak is dominated by interaction induced effects and that these effects cannot be neglected as stated in the last section. The difference between the response calculated using the DID model with that of the POL model shows that the multipole effects are also quite important. The difference between the POL and DRF results is limited, showing the smaller influence of the close collision electron overlap effects. This is also what could be expected from the comparisons made in chapter 5.

In Figure 7.3 the same responses are shown but now normalized to peak height and together with the experimental response obtained by Steffen *et al.* [82] When plotted in this way the DID, POL and DRF models all look very similar to the experimental response in the subpicosecond peak area. In the long tail the DID response is somewhat lower than the experimental response whereas the POL and DRF are higher. This means that the DID model overestimates the ratio between the interaction induced effects and the single molecule response, and the POL and DRF models underestimate this ratio to a much lesser

FIGURE 7.2: *The anisotropic third-order Raman response of liquid CS_2 in units of* 10^{-20} C^4m/J^3s.

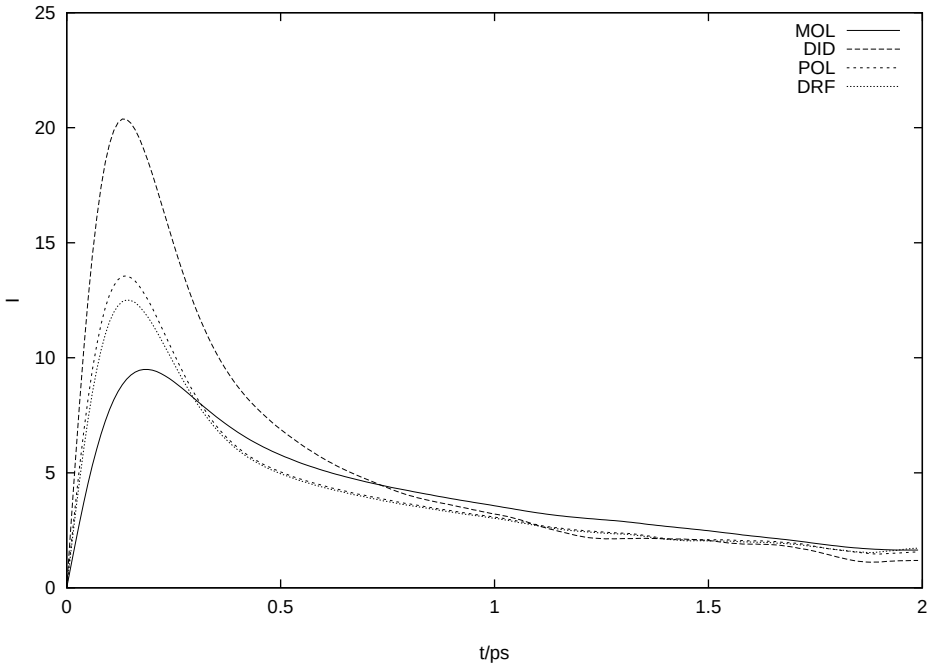

extent.

In Figure 7.4 the isotropic responses are shown. The single molecule contribution to this component is zero, so all response is originating from the interaction induced many-body effects. Note that these signals are about an order of magnitude or more weaker than the anisotropic response shown in Figure 7.2. A large difference is observed between the DID model and the models including multipole effects. Again the DID model is overestimating the interaction induced response. From this substantial difference it must be concluded that the induced multipole effects should be included when one calculates especially the isotropic third-order response. Unfortunately there are no reliable experimental results to compare with since the intensity is much smaller than the anisotropic response. Measurements by Blank *et al.* [74] just showed a very weak shoulder on the electronic response, but more recent measurements [64, 175, 184, 185] show promise for a more accurate measurement of the isotropic response.

To give a quantitative comparison between the different calculations the responses have been fitted to the functions given in Eqs. (3.30) and (3.31). In these fits it is assumed that the shape of the single molecule response is not dependent on the model used to describe

FIGURE 7.3: *The anisotropic third-order Raman response of liquid CS_2 normalized to one at the peak position.*

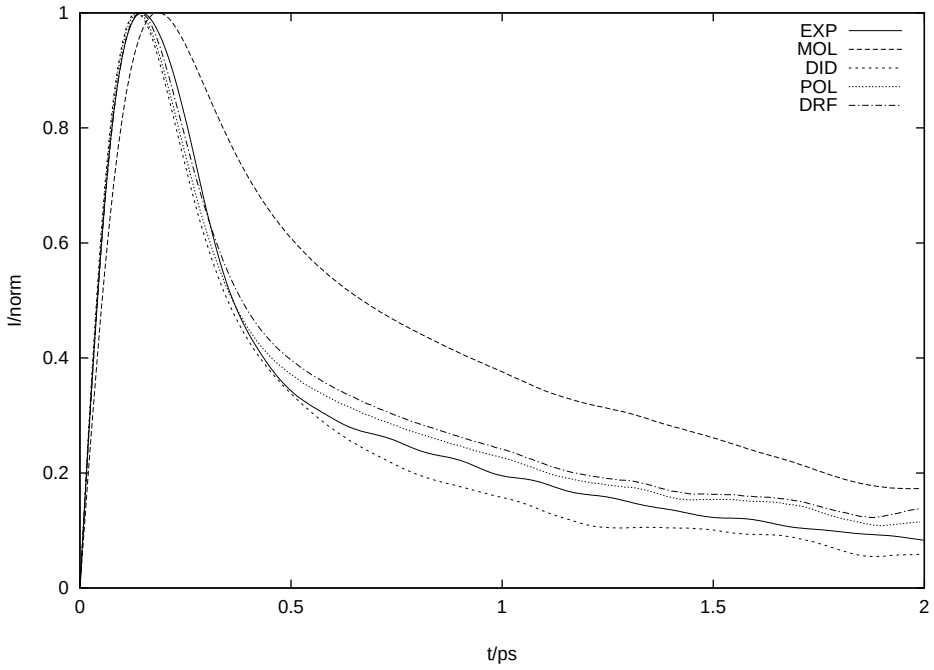

the interaction induced effects. The results are shown in Table 7.1. The single molecule (MOL) response has been fitted to Eq. (3.30) and the fit constants τ_D, τ_R, A_R, Ω_R and w_R that determine the shape of the single molecule response are kept fixed for the fits to the DID, POL and DRF results, while the constant I_D that determine the intensity is allowed to vary. No single molecule response is present in the isotropic response. From these fits it is clear that for the anisotropic response there is a big difference between the DID model and the models including the multipole effect. This is seen both in the I_C parameter characterizing the intensity and the τ_C and n parameters characterizing the shape of the interaction induced response. For the isotropic response the main difference is in the parameter characterizing the intensity. The ratio between the peak intensity of the anisotropic and the isotropic response changes dramatically from 7.57 in the DID model to 21.0 in the DRF model. These ratios provide a sensitive test of these models that can be determined experimentally.

For the single molecule response the librational part is found to be close to critically damped while the A_R and Ω_R parameters can be varied quite a bit without changing the function too much, as long as the product of these two constants is kept fixed. The

TABLE 7.1: *The fit constants for the calculated single molecule (Eq. 3.30) and interaction induced (Eq. 3.31) response, with I_D and I_C giving the intensities. No single molecule response is present in the isotropic response which is therefore fitted to the interaction induced expression (Eq. 3.31) with I_C as intensity.*

	Anisotropic									Isotropic		
	Single Molecule					Inter. Ind.			Inter. Ind.			
	I_D	τ_D	τ_R	A_R	Ω_R	w_R	I_C	τ_C	n	I_C	τ_C	n
MOL	8.32	1.20	0.117	6.19	0.803	31.7	-	-	-	-	-	-
DID	5.88	−||−	−||−	−||−	−||−	−||−	22.26	0.183	1.83	4.506	0.156	1.53
POL	7.39	−||−	−||−	−||−	−||−	−||−	8.09	0.306	3.06	1.312	0.137	1.50
DRF	7.26	−||−	−||−	−||−	−||−	−||−	6.66	0.309	3.09	0.985	0.165	1.63

FIGURE 7.4*: The isotropic third-order Raman response of liquid CS_2 in units of* 10^{-20} C^4m/J^3s*. The response in molecular polarization model (MOL) is zero.*

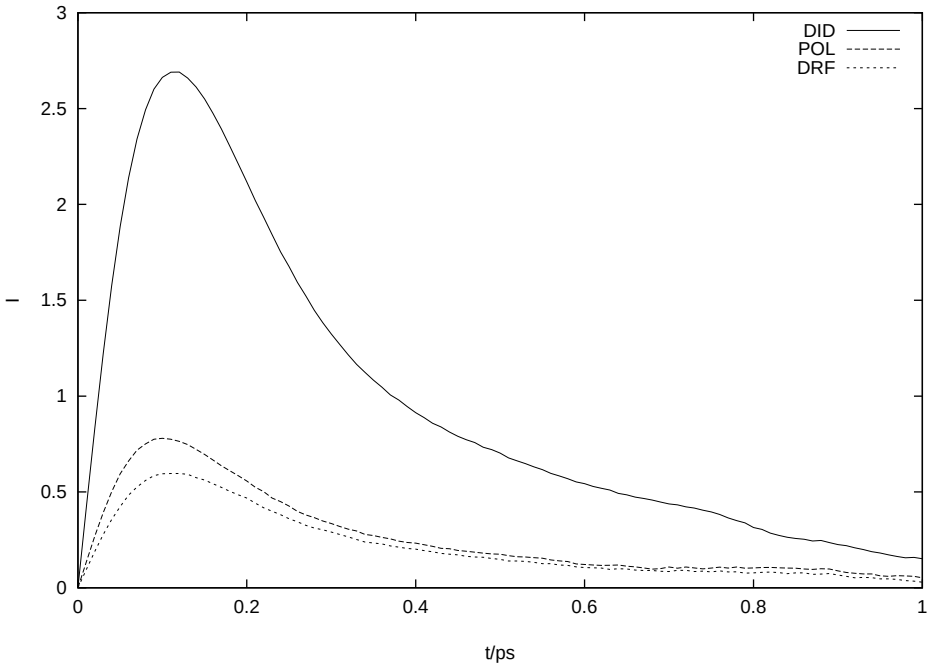

diffusional constant τ_D is found to be 1.20 ps, which is somewhat lower than the value 1.6 ps typically reported. [69,117,120,121,174] This is probably an artifact due to the truncation of the calculated response at 2 ps. The long tail domain is not really included in the simulation. This gives an uncertainty in the diffusional constant τ_D that may be partly due to compensation of the errors in the librational part of the response. The calculated third-order response was found to resemble the experimental result very well.

The observed rather small deviation between the response calculated using the DRF method and the experimental response does not need to originate only from the small remaining differences between the modeled and calculated polarizabilities. The fact that the force field used in the MD simulations is rather simple (as described in chapter 6) can also give rise to deviations. A molecular force field consisting of isotropic atomic Lennard-Jones potentials cannot give rise to the anisotropic asymptotical behavior that is present in anisotropic molecules as CS_2, but only mimics the anisotropy in the force field at short distances [165]. Furthermore, in the force field used the relatively large quadrupole moment in CS_2 is not taken into account. Test calculations showed that omitting the partial charges has little effect and the partial charges have not been included in order to allow comparison

with earlier studies where charges were also discarded.

The interaction induced effects observed for the third-order response will surely also have implications on the calculated higher (fifth) order Raman response, which is known to be even more sensitive to many-body effects in the optical response [56, 87, 103].

7.3 Molecular fifth-order response

The fifth-order response was first calculated [55] using the molecular model for the polarizability (MOL). This is done by averaging over 8000 finite field simulations with a duration of 0.75 ps. The strength of the applied laser fields was 0.383 V/Å. The result is shown in Figure 7.5. To give an indication of the noise introduced by the perturbation of the system, the spread on the mean value of the response function at each time t_2 is also plotted in Figure 7.5 for the calculation with t_1=0.2 ps. The peak intensity was found to be 0.98 $\times 10^{-25}$ C^6m^3/J^5s^2 which occurs for t_1=0.2 ps and t_2=0.2 ps.

FIGURE 7.5: *Fifth-order response* $\chi^{(5)}_{zzzzzz}$*, calculated using the finite field method. The different lines correspond to different values of* t_1*, with* t_1 *increasing from 0.1* ps *in the left trace to 0.7* ps *in the right trace in steps of 0.1* ps*. The positively inclined line at the bottom signifies the noise level in the calculation with* t_1*=0.2* ps*.*

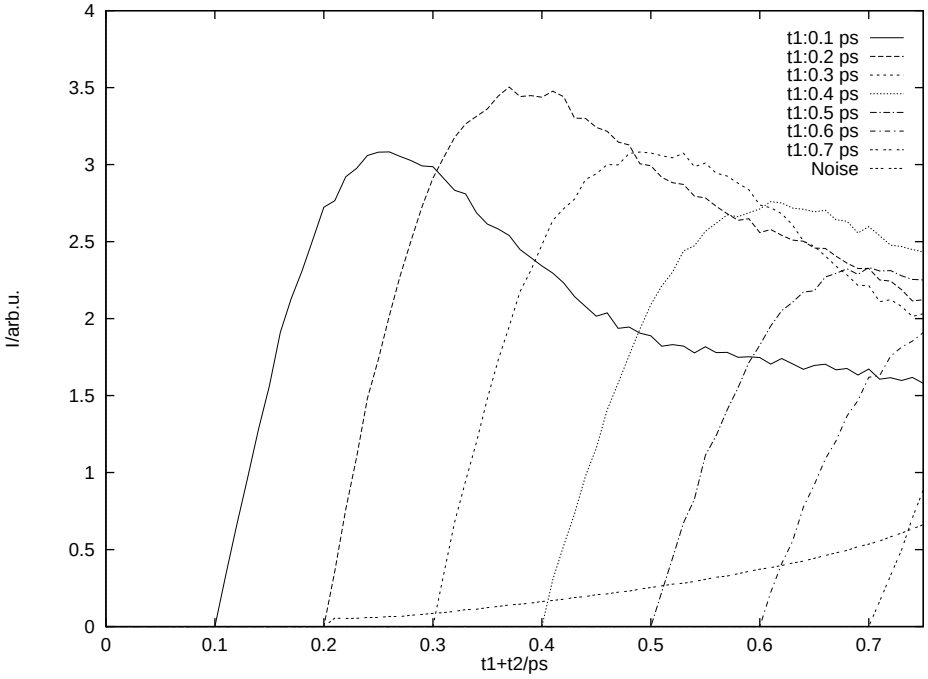

The intensity ratio of the cascaded and fifth-order response can be estimated from the peak values of the third- and fifth-order response functions in the sample. Using the calculated response function peak intensities, the experiment independent ratio (Eq. (2.34)) is found to be 0.0104 in the MOL model. With this information Eq. (2.33) gives an approximate intensity ratio of the two types of response of 4×10^6 in favour of the third-order cascade processes when a wavelength of 620 nm, a sample size of 1 mm and perfect phase matching, $f(\Delta kl) = 1$ is taken. This indicates that the cascade process should be very severely mismatched in phase under experimental conditions, in order to be able to observe the two-dimensional fifth-order Raman signal. Such mismatch was not present in most experiments reported so far [38–41], but recent multi-color experiments have increased the phase mismatch considerably. Possibly the discrimination against cascaded processes is then sufficiently to isolate the true fitfh-order response. [43–45]

The estimated intensity ratio of 4 million between the 3rd-order cascading processes and the true fifth-order response, in favour of the cascading processes before taking phase matching into account, supports the conclusions of Blank *et al.* [41] that all earlier reported experimental results of two-dimensional Raman scattering actually dealt with cascading processes, instead.

7.4 Fifth-order DID response

The time dependence and intensity ratio against the cascaded processes was calculated in the previous section for a sample of independent molecules. Interaction induced effects may modify these results considerably. Therefore, the fifth-order response including the dipole induced-dipole (DID) contribution was calculated. This was done by applying the finite field method with 1000 simulations for each of the four combinations of applied laser fields shown in Eq. (3.2) and for t_1 values from 20 fs to 200 fs in 20 fs steps and t_2 values from 0 to 200 fs in 10 fs steps. The strength of the applied laser fields was 1.149 V/Å. All calculated tensor components were obtained from two sets of trajectories that differ in the polarization directions of the laser fields: one that has the polarization direction of the first laser pulse pair along the z-axis and one that has the polarization direction of the first laser pulse pair along the y-axis. The laser pulse pair applied after the delay t_1 is always applied with the polarization direction along the z-axis. The zz component and the yy component of the first-order susceptibility are calculated after the delay t_2. This provides the $\chi^{(5)}_{zzzzzz}$, $\chi^{(5)}_{zzzzyy}$, and $\chi^{(5)}_{zzyyzz}$ components, from which the desired $\chi^{(5)}_{zzzzzz}$, $\chi^{(5)}_{mmzzzz}$, $\chi^{(5)}_{zzmmzz}$, $\chi^{(5)}_{zzzzmm}$ and

$\chi^{(5)}_{llzzl'l'}$ tensor elements can be calculated as also mentioned in chapter 3. These calculated components are shown in Figure 7.6. Cuts through the surfaces along the diagonal and for t_2 fixed at 120 fs are shown for the different components in Figure 7.7 and Figure 7.8. In Table 7.2 the peak intensities are given and in Table 7.3 the peak positions of the cascading processes and the calculated fifth-order response are listed together with the experimental positions given by Blank *et al.* [74] Table 7.4 contains the experiment-independent intensity ratios as defined in Eq. (2.34). Assuming an experimental wavelength of 620 nm, a sample length of 1 mm and perfect phase matching conditions, Δkl , the experimental factor is 3.9×10^8 (Eq. (2.35)). In the experiments performed by Blank *et al.* [74] a wavelength of 800 nm is used, which favours the true response with a factor of 1.6 in comparison with the conditions considered here.

TABLE 7.2*: Peak values for the calculated response functions using the finite field method (FF) and the time correlation function method (TCF) when possible. Third-order values are given in units of* 10^{-20} C^4m/J^3s *and the fifth-order values in units of* 10^{-25} C^6m^3/J^5s^2. *(For comparison with data in c.g.s. units: 1* e.s.u. *(or* cm^3*)*$= 1.11264\times10^{-16}C^2m^2J^{-1}$, 1 erg $= 10^{-7}$ J *and* 1 $C^4m/J^3s = 8.07761\times10^6cm^3erg^{-1}ps^{-1}$)

$\chi^{(n)}_{a\cdots b}$	FF	TCF	Deviation
$\chi^{(3)}_{zzzz}$	28.59	28.28	1.1 %
$\chi^{(3)}_{zzmm}$	2.37	2.40	-1.2 %
$\chi^{(3)}_{zyzy}$	19.73	19.21	2.7 %
$\chi^{(3)}_{zzll}$	-1.12	-1.10	-.18 %
$\chi^{(5)}_{zzzzzz}$	0.107	-	-
$\chi^{(5)}_{mmzzzz}$	0.0327	-	-
$\chi^{(5)}_{zzmmzz}$	0.0481	-	-
$\chi^{(5)}_{zzzzmm}$	0.0346	-	-
$\chi^{(5)}_{llzzl'l'}$	-0.0252	-	-

The case least discriminating against cascaded processes is the $\chi^{(5)}_{zzzzzz}$ response, where the intensity ratio between the most intense cascaded signal and the true fifth-order response becomes 2.8×10^6 in favor of the cascading processes, when the experimental factor above is used. In the last section, where the local field effects were not included, this ratio was found to be 4×10^6. For the magic angle component $\chi^{(5)}_{zzmmzz}$ the intensity ratio for the parallel cascaded response is found to be 9.8×10^4. For the $\chi^{(5)}_{llzzl'l'}$ response this ratio

FIGURE 7.6*: Five polarization components of the fifth-order response of carbon disulfide calculated using the finite field method. The plots are made with ten equidistant contour lines.*

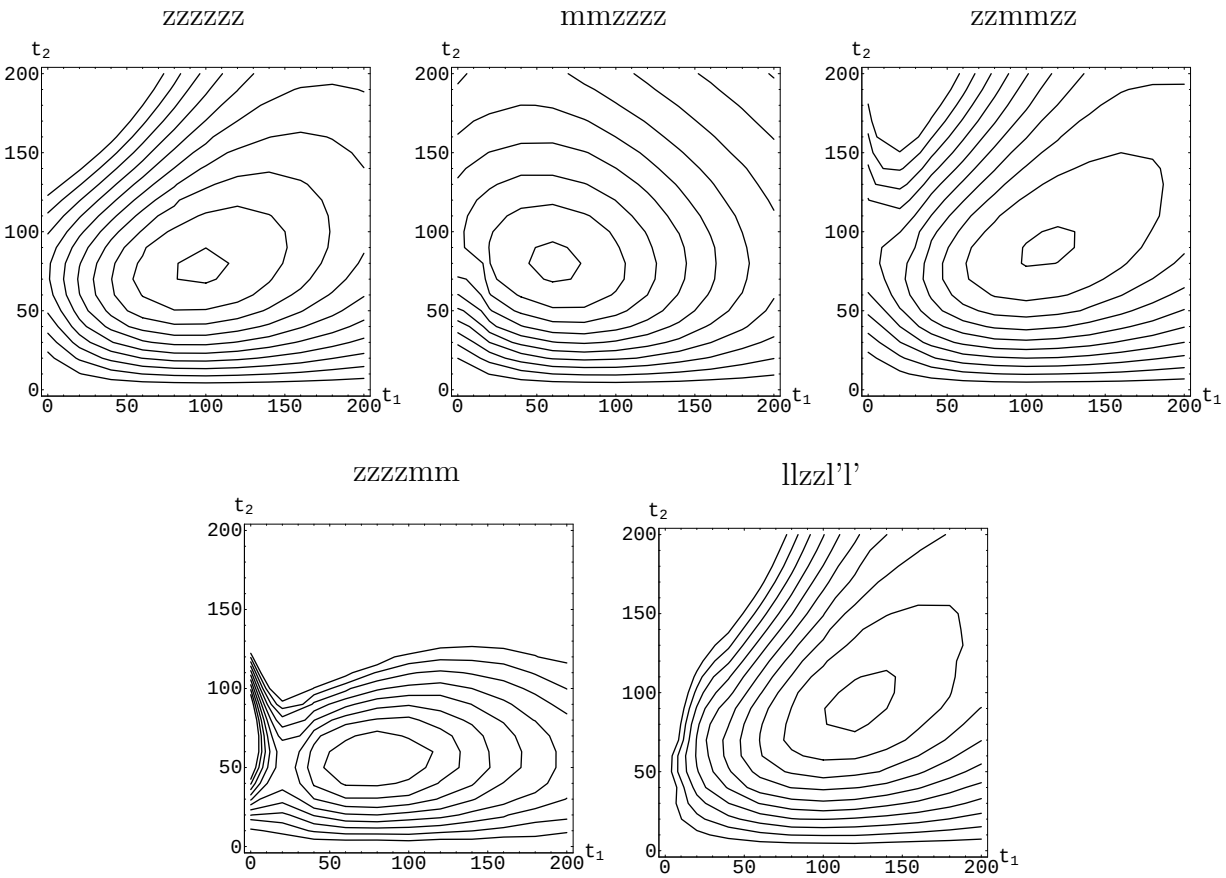

FIGURE 7.7: *Diagonal cut through the two-dimensional fifth-order response surfaces. The full line is the $\chi^{(5)}_{zzzzzz}$ component, the dotted line is the $\chi^{(5)}_{mmzzzz}$ component, the dashed line is the $\chi^{(5)}_{zzmmzz}$ component, the long dashed line is the $\chi^{(5)}_{zzzzmm}$ component, and the dashed-dotted line is the $\chi^{(5)}_{llzzl'l'}$ component. The response is given in units of $10^{-25}\mathrm{C}^6\mathrm{m}^3/\mathrm{J}^5\mathrm{s}^2$.*

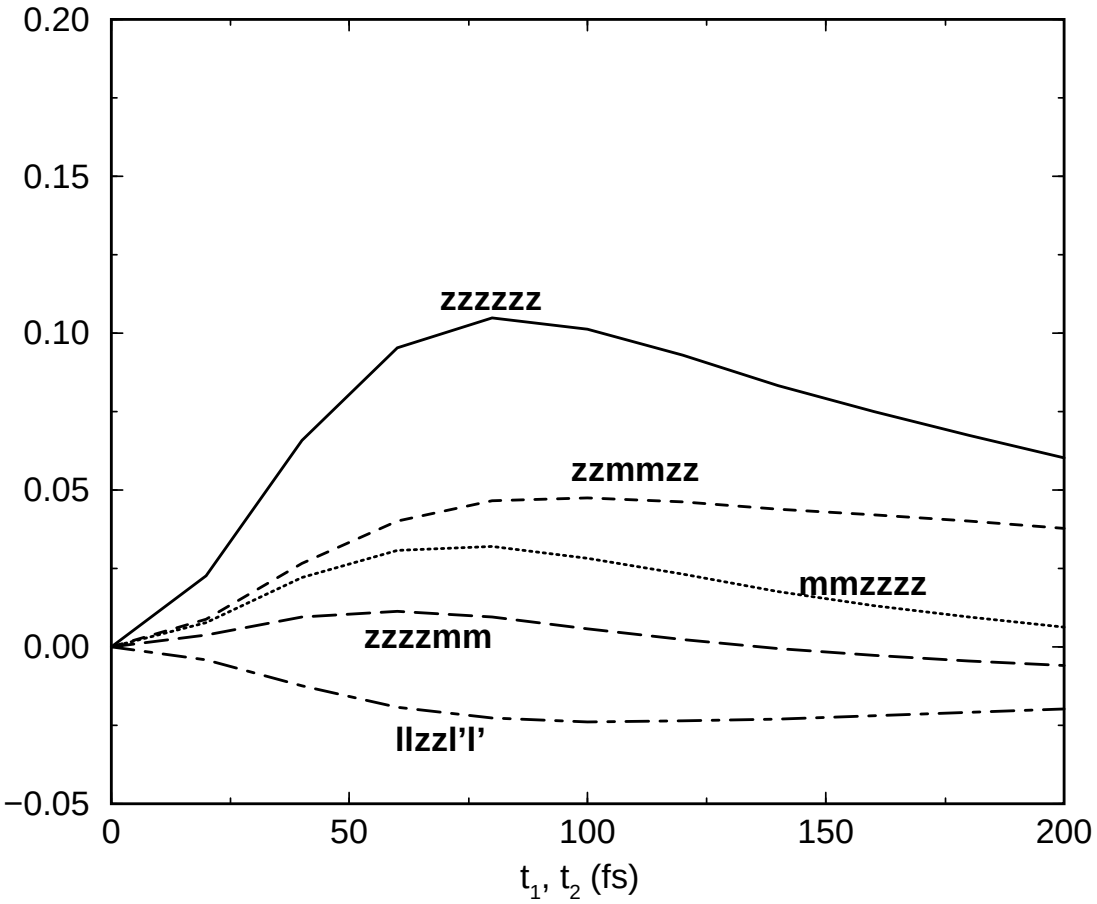

FIGURE 7.8*: Cut through the two-dimensional fifth-order response surfaces with t_2 fixed at 120* fs*. The full line is the $\chi^{(5)}_{zzzzzz}$ component, the dotted line is the $\chi^{(5)}_{mmzzzz}$ component, the dashed line is the $\chi^{(5)}_{zzmmzz}$ component, the long dashed line is the $\chi^{(5)}_{zzzzmm}$ component, and the dashed-dotted line is the $\chi^{(5)}_{llzzl'l'}$ component. The response is given in units of* $10^{-25}\mathrm{C}^6\mathrm{m}^3/\mathrm{J}^5\mathrm{s}^2$.

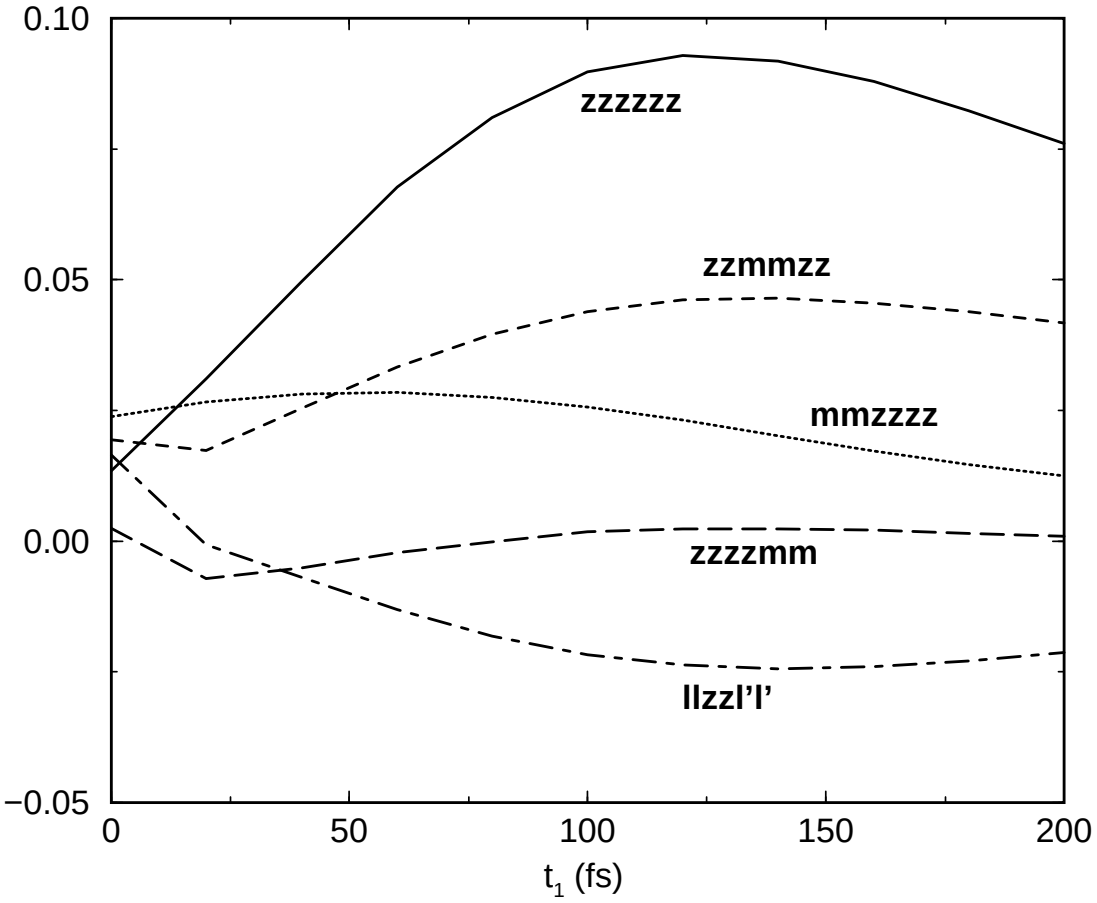

TABLE 7.3: *Peak positions for the direct fifth-order response and the cascading response compared with the experimental results of Blank et al. [74] The peak positions are given as* (t_1, t_2) *in units of* fs.

$\chi^{(5)}_{abcdef}$	$\chi^{(5)}_{abcdef}$	$\chi^{(5)}_{\mathrm{seq}}$	$\chi^{(5)}_{\mathrm{par}}$	Exp.
$\chi^{(5)}_{zzzzzz}$	(100,80)	(140,140)	(0,140)	(60,110)
$\chi^{(5)}_{mmzzzz}$	(60,80)	(140,110)	(0,110)	-
$\chi^{(5)}_{zzmmzz}$	(100,90)	(110,110)	(-30,110)	-
$\chi^{(5)}_{zzzzmm}$	(80,50)	(110,140)	(30,140)	(0,120)
$\chi^{(5)}_{llzzl'l'}$	(120,90)	(200,200)	(0,200)	-

TABLE 7.4: *Experimental independent intensity ratios between the peaks of the cascaded response and the fifth-order response for the different polarization components.*

$\chi^{(5)}_{abcdef}$	R_{seq}	R_{par}
$\chi^{(5)}_{zzzzzz}$	7.2×10^{-3}	7.2×10^{-3}
$\chi^{(5)}_{mmzzzz}$	5.3×10^{-4}	3.7×10^{-6}
$\chi^{(5)}_{zzmmzz}$	1.7×10^{-6}	2.5×10^{-4}
$\chi^{(5)}_{zzzzmm}$	4.7×10^{-4}	4.7×10^{-4}
$\chi^{(5)}_{llzzl'l'}$	3.1×10^{-7}	3.1×10^{-7}

is only 1.2×10^2, which allows to discriminate against the cascaded response, when the intermediate phase matching factor is better than 1×10^3. This is the order of magnitude reported experimentally [74].

The fifth-order magic tensor elements $\chi^{(5)}_{mmzzzz}$, $\chi^{(5)}_{zzmmzz}$ and $\chi^{(5)}_{zzzzmm}$ are all approximately three times smaller than the $\chi^{(5)}_{zzzzzz}$ component. The ratio between the polarized and magic angle components in the third-order experiment is approximately 12 in favor of the polarized component. This implies that the isotropic part of the response, which cannot be explained without interaction induced effects, is much stronger in the fifth-order response than in the third-order response. The sensitivity of the fifth-order response to many-body effects, found here, was recently also inferred from INM calculations by Murry *et al.* [87] This probably also means that the fifth-order signal is more sensitive to other interaction induced effects than the DID effect accounted for here. The induced multipoles, described in chapter 2, are very likely to give a significant contribution to the fifth-order response. This will be treated in the following section.

The differences between the nuclear part of the experimental signal [74] and the calculated response are pronounced. Both the $\chi^{(5)}_{zzzzzz}$ and the $\chi^{(5)}_{zzzzmm}$ component of the experimental response have sharp peaks closer to the t_2-axis than shown in the rather flat calculated two-dimensional surfaces of Figure 7.6. This probably indicates that the signals are contaminated with parallel cascaded response that peaks on or close to the axis.

Comparing the calculated and experimental response is complicated by the fact that the experimental signals may include contributions from combined electronic/nuclear response along the time axes and pure electronic response for both time delays equal to zero. [72] These responses depend on the higher order non-linear electronic responses γ and ζ (or the macroscopic electronic counterparts $\chi^{(3)}$ and $\chi^{(5)}$) respectively as shown in section 2.2. Since they are confined to the origin and the time axes, problems with separating nuclear and electronic response are limited to these areas. In addition the experimental spectra are broadened by the width of the applied laser pulses. This experimental artifact is best corrected for by deconvoluting the experimental response before comparing it with the calculated ideal response using delta function pulses. Recently a method for doing this with the fifth-order homodyne detected response has been published. [83]

The estimated ratios between the cascaded processes and the direct fifth-order response are in favor of the cascaded processes, even when the experimental factor in Eq. (2.35) with a realistic phase matching factor is taken into account. However, the ratio is smaller than in studies not taking the local field effects into account [55] and for the $\chi^{(5)}_{llzzl'l'}$ component

the ratio is close to one. This again indicates the importance of interaction induced effects in the fifth-order response. The calculations still support the conclusion by Blank *et al.* [41] that all experiments performed earlier are dominated by the cascaded processes.

In the light of the recent experiments, that were claimed to contain direct fifth-order response, [74] it seems that the theory overestimates the intensity ratios or that the experiment overestimates the mismatch in the intermediate phase matching factors. The experimental factor might be connected with uncertainties concerning, for instance, the beam divergence or the sample length, which is not only determined by the sample thickness, but also by the overlap of the laser beams. [41] The estimated intermediate phase matching conditions, discriminating the fifth-order signals against the third-order cascaded response, is also not fully determined due to uncertainty in the orientation of the laser beams. On the other hand, the interaction induced effects might be calculated more accurately by including higher order terms in the multipole expansion and/or collision induced contributions [62] as will be done in the following section.

7.5 Fifth-order DRF response

In the third-order Raman response the inclusion of induced multipole effects and electron overlap were found to be important. The fifth-order response is more sensitive to the detailed coordinate dependence of the first-order susceptibility and therefore the induced multipole effects and the electron overlap can be expected to be even more important in the fifth-order response than in the third-order response.

To obtain the highest accuracy in the calculations, the inverted force variant of the finite field method described in chapter 3 was applied in the calculation of the fifth-order response with the DRF model. This allowed using a laser strength of 1.915 V/Å without introducing higher order artifacts. The calculations were performed on a simulation box with 64 molecules and repeated for 4000 different starting configurations. The response was calculated for times t_1 and t_2 between 0 and 600 fs, with a 20 fs resolution. For comparison the MOL, DID and POL model responses were also calculated under the same conditions, but with a slightly lower laser strength of 1.724 V/Å for the MOL and DID models. In the DID calculations only 2000 starting configurations were needed. The calculated responses for the $\chi^{(5)}_{zzzzzz}$ and $\chi^{(5)}_{mmzzzz}$ polarization directions are shown in Figure 7.9 and Figure 7.10.

For the $\chi^{(5)}_{zzzzzz}$ component the molecular response is somewhat elongated along the t_2

axis. The response found with the DID model including intermolecular interactions is more symmetric, while the POL and DRF model responses are even more stretched out along the t_2 axis than the pure molecular response. In the third-order response the induced multipoles were seen to damp the effect of the dipole-induced dipoles. This also seems to be the case in the fifth-order response, but in fifth-order the POL model stretches the response even more along the t_2 axis than the molecular model does. Furthermore, slight differences are also observed between the POL and DRF model responses showing that electron cloud overlap is of some importance.

In the $\chi^{(5)}_{mmzzzz}$ response the signal is independent of the individual molecular orientations and the molecular polarizability model does not give rise to optical response. The differences between the DID, POL and DRF models along the t_2 axis are even more pronounced for this component, as shown in Figure 7.10. The DID model response is rather symmetrical, while the POL and DRF model responses shows a ridge along the t_2 axis. This clearly shows that the multipole effect is also of crucial importance in the fifth-order response. The effect of electron cloud overlap is clearly visible in the area where t_1 and t_2 are 100 fs. A clear peak is seen in the DID and POL models, while this is not observable in the DRF model response where the electron overlap is taken into account.

At the present moment we can only speculate on the interpretation of the spectrum. The long ridges along the t_2-axis can possibly be explained by a model suggested by Steffen and Duppen [186] involving population relaxation during the second time delay. However, the response is more complicated than that. It is essential to understand why the DID response is rather symmetric while the DRF response is highly assymetric. The only difference between these two models is the distance and orientation dependence of the polarizability, as reported in chapter 5. There it was shown that the polarizability at short intermolecular distances was damped in the DRF model. This means that the contribution to the response from molecules at short separations is smaller in the DRF model than in the DID model. This could indicate that dimers at short separations are responsible for the rather symmetric part of the response, while dimers at larger separations give rise to the response along the axis. It is reasonable that the shape and nature of the response depends on the distance between the molecules, since the intermolecular forces they experience will be much different. More investigations will be needed to give an exact interpretation of the spectral features.

The multi-color experiments published recently [45,187,188] were claimed to be in good qualitative agreement with the results reported in last section. Some of these experimental

FIGURE 7.9: *The calculated fifth-order response $\chi^{(5)}_{zzzzzz}$ with the MOL, DID, POL and DRF models for the first-order susceptibility. The plots are made with ten equidistant contour lines.*

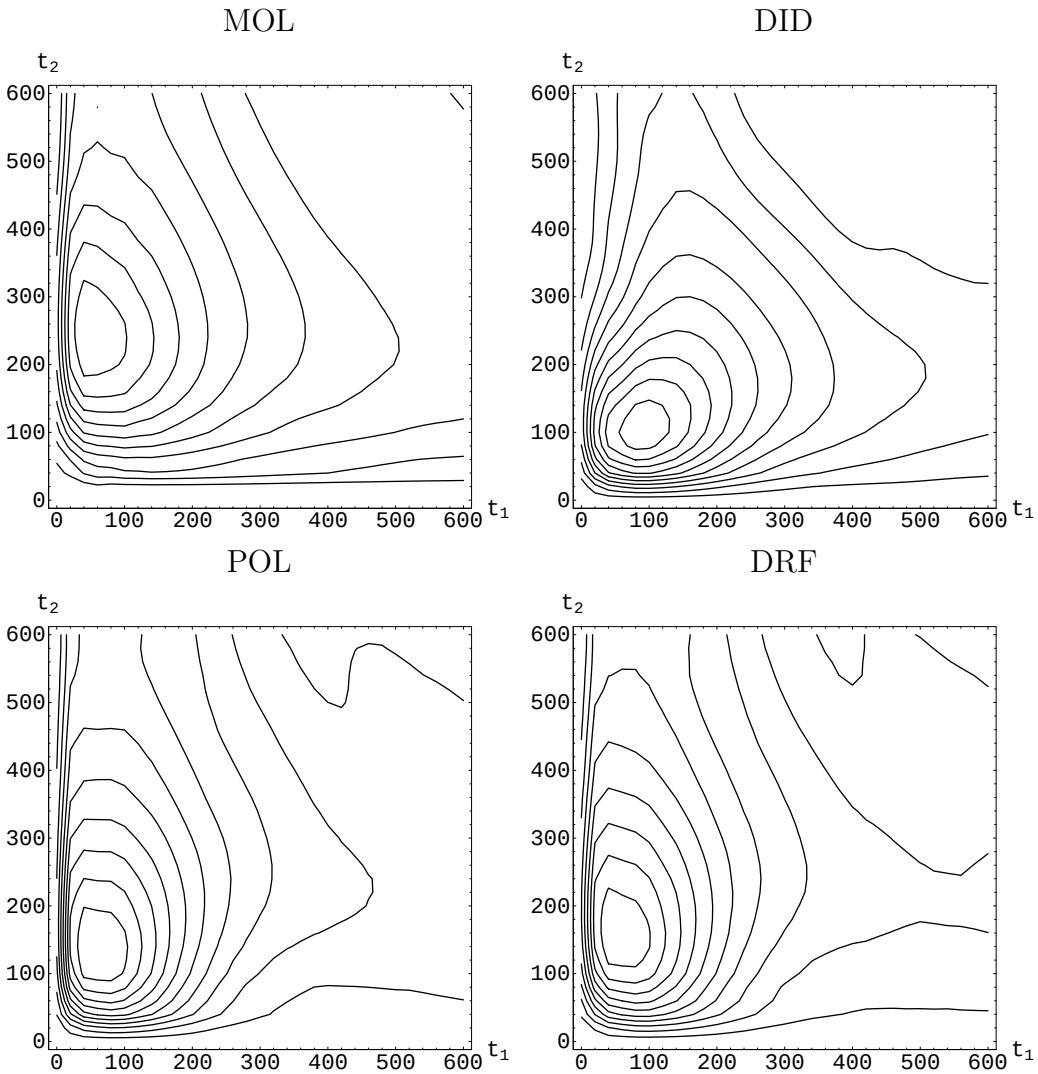

FIGURE 7.10: *The calculated fifth-order response $\chi^{(5)}_{mmzzzz}$ with the DID, POL and DRF models for the first-order susceptibility. In the MOL model this response vanishes. The plots are made with ten equidistant contour lines.*

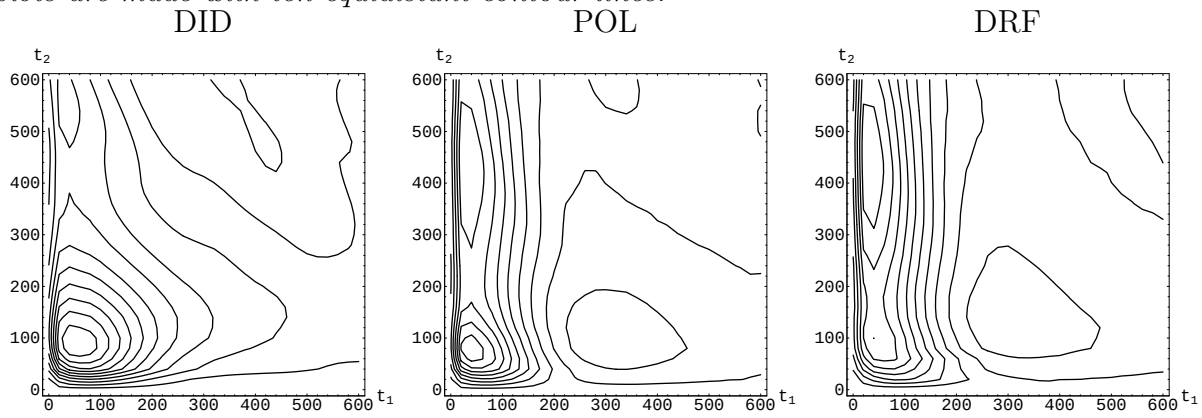

results can be seen in Figure 7.11. In these experiments the cascaded processes are severely suppressed by the phase mismatch. For the $\chi^{(5)}_{zzzzzz}$ component shown in Figure 7.11 a long tail along the t_2 (τ_4) axis is observed in agreement with the response calculated with the DRF model. Since only cuts through the two-dimensional surface have been presented with this experimental method, a more detailed comparison is impossible.

In recent theoretical [101] and experimental studies [189] nodal lines in the $\chi^{(5)}_{zzzzzz}$ response of CS_2 were reported. Such features are not observed in the multi-color experiments by Kubarych [45,187,188] nor in the present simulations. In the DID response reported in section 7.4 the response indeed becomes slightly negative along the t_2-axis for the $\chi^{(5)}_{zzzzzz}$ component, when t_2 is large, but this has been identified as an artifact due to higher-order response. This artifact was eliminated in the later simulations by applying the inverted force approach.

7.6 Conclusion

Since the instantaneous normal mode calculations [58, 87, 103, 106] lack the ability to describe diffusive motion, and the time correlation function response can in fifth-order only be done on very small systems, [59, 101] the finite field approach is the most promising method for further applications. The finite field method was shown to give the same third-order response as the time correlation function method, giving confidence that the method

FIGURE 7.11: *The experimental response reported by Kubarych et al. [45]. The full lines are the in-phase signal (dominated by true response), while the dotted lines are the in-quadrature signal (dominated by cascades). Cuts through the two-dimensional surface are shown along the t_2 (τ_4) axis, along the t_1 (τ_2) axis and along the diagonal (shown from top to bottom). The $\chi^{(5)}_{zzzzzz}$, $\chi^{(5)}_{zyzzzy}$ and $\chi^{(5)}_{zzmmzz}$ components are shown from left to right.*

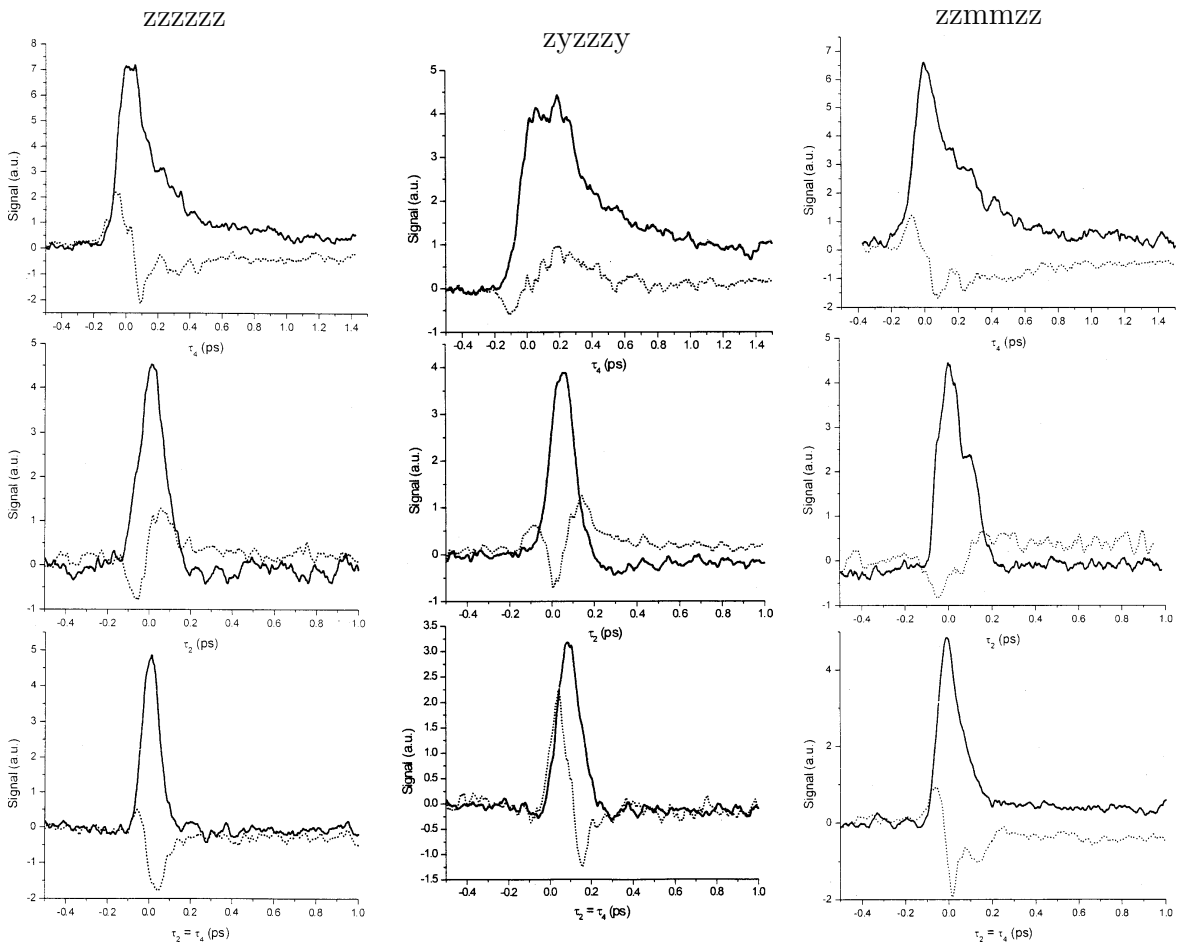

is reliable. This method makes it possible to provide reasonable estimates of the relative intensity of the true fifth-order response and the competing third-order cascades.

This study showed that close collision effects caused by induced multipoles and electron cloud overlap are crucial for giving a correct description of both the third- and fifth-order response. The close collision effects are most important in the isotropic third-order and fifth-order responses, where the difference between the results calculated with the different polarizability models are most pronounced. This proves that fifth-order response is a strong tool for investigating these close collision effects as well as the intermolecular motion giving rise to the many-body response.

Still further research is required in order to give a clear interpretation of the spectra and in order to establish a clear consensus between the experimental and theoretical results. This will allow fifth-order Raman spectroscopy to become a useful method for studying the complicated motion of liquids.